

Low permeability composite magnetic core transformer with high coupling coefficient and its application to PFM controlled quasi-resonant mode flyback-type DC-DC converter

K. Sato^{*,**}, T. Sato^{**}, M. Sonehara^{**}, and H. Takeuchi^{*}

^{*}Nagano Prefecture General Industrial Technology Center, 1-3-1 Osachi-katamacho, Okaya, Nagano 394-0084, Japan

^{**} Faculty of Engineering, Shinshu Univ., 4-17-1 Wakasato, Nagano, Nagano 380-0928, Japan

We describe a low permeability composite magnetic core transformer with a high coupling coefficient and its application to a PFM controlled quasi-resonant mode flyback-type DC-DC converter. To increase the coupling coefficient between primary and secondary windings embedded in a carbonyl-iron powder/epoxy composite magnetic core with a relative permeability of 6, three types of winding layouts were investigated by using a 2D-FEA numerical simulation and the characteristics were confirmed experimentally. The primary and secondary windings that were laid out adjacent to each other were the best choice as it had the highest coupling coefficient at over 0.99. By applying the composite magnetic core transformer with this coupling coefficient to a 48 V input/12 V output PFM controlled quasi-resonant mode flyback-type DC-DC converter, the maximum efficiency was 92.5% at an output power of around 28 W, and an efficiency of 90.0% was obtained at an output power of 60 W.

Key words: low permeability magnetic core, carbonyl-iron powder/epoxy composite magnetic core transformer, winding layout, coupling coefficient, DC-DC converter, efficiency

1. Introduction

Recently, SiC/GaN power devices have been applied to switching power converters. It is because they make possible to have good advantages such as lower ON resistance, higher speed switching operation and higher temperature operation than the Si-based power devices^{1), 2)}. By using the novel power devices, it is possible not only to increase the power conversion efficiency of the converter but also to downsize the magnetic devices used in the switching power converters since the switching frequency can be increased to MHz band or tens of MHz. However, it is considered difficult to use the magnetic devices consisting of dust core or Mn-Zn ferrite core for such the very high frequency switching power converter. M. Harrison³⁾ stated that the possible magnetic core for MHz band or beyond 10 MHz power conversion would be Ni-Zn ferrite core only.

The authors are developing a novel magnetic core as a candidate substitute for the Ni-Zn ferrite core, for example, the carbonyl-iron powder/epoxy composite magnetic core was developed⁴⁾ and was applied to switching power converters^{5), 6)}. In order to increase the volume resistivity of the composite magnetic core body, the surface-oxidation for the carbonyl-iron powder was very effective⁴⁾. Though the surface-oxidized carbonyl-iron powder/epoxy composite magnetic core had a low relative permeability of about 6, the magnetic loss was very small up to 10 MHz in frequency. By applying the composite magnetic core inductor to a 1 MHz switching buck-type DC-DC converter using GaN power device, a maximum power conversion efficiency of 93% was obtained⁵⁾. It was also reported that a composite magnetic core transformer with copper-clad polyimide tape windings embedded in the composite

magnetic core could realize a coupling coefficient $k > 0.99$ even when using such the low permeability composite magnetic core⁶⁾. Furthermore, by applying the composite magnetic core transformer to a PWM (Pulse Width Modulation) controlled flyback-type DC-DC converter, the maximum power conversion efficiency was 91% at 400 kHz switching and 85% at 1 MHz switching⁶⁾.

In general, the low permeability magnetic material is not suitable for transformer core because of large leakage inductance owing to the low coupling coefficient between the windings. This study was done to develop the composite magnetic core transformer with high coupling coefficient and to apply it to a PFM (Pulse Frequency Modulation) controlled quasi-resonant mode flyback-type DC-DC converter⁷⁾.

This paper describes an investigation on the design of low permeability composite magnetic core transformer with high coupling coefficient on the bases of the two-dimensional finite element analysis (2D-FEA) numerical simulation and experiments. In addition, a PFM controlled quasi-resonant mode flyback-type DC-DC converter using the fabricated composite magnetic core transformer is also shown.

2. Surface-oxidized carbonyl-iron powder/epoxy composite magnetic core transformer

2.1 Properties of surface-oxidized carbonyl-iron powder/epoxy composite magnetic core

As the soft magnetic metal powder for the composite magnetic core, non-reduction carbonyl-iron powder with a mean diameter of 1.6 μm was used. In order to prevent the electrical contact between the adjacent powders in the composite magnetic core and to

suppress the over-lapped eddy current loss, high resistive oxidized layer of several tens of nm was introduced on the surface of the powders by thermal oxidation in air at 200 degrees-C for 6h⁴⁾. The composite magnetic core was fabricated by the casting and post-curing using the composite slurry with the surface-oxidized carbonyl-iron powder and epoxy precursor solution. Since the nonmagnetic epoxy resin between the magnetic particles behaves as a magnetic gap, the composite magnetic core is hard to be magnetically saturated due to its low permeability and has superior superimposed DC current characteristics when using the magnetic devices, so that the transformer core can be gapless.

Fig. 1 shows the static magnetization curve of the surface-oxidized carbonyl-iron powder/epoxy composite magnetic core measured by using a VSM (Riken Denshi Co., Ltd.; BHV-55). The saturation magnetization was about 1 T. Though the composite magnetic core had nonmagnetic epoxy resin, it exhibited a high saturation magnetization around 1 T, so it was considered that the energy density could be increased and the transformer core could be downsized.

Fig. 2 shows the frequency dependence of the relative complex permeability of the surface-oxidized carbonyl-iron powder/epoxy composite magnetic core measured by using an impedance/material analyzer

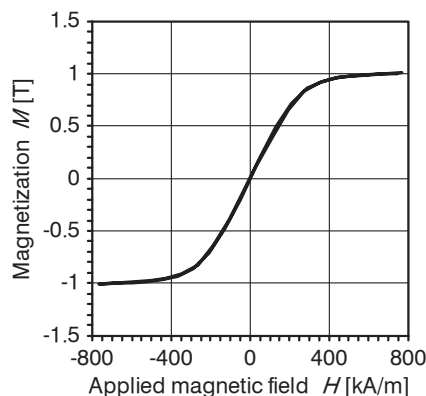


Fig. 1 Static magnetization curve of surface-oxidized carbonyl-iron powder/epoxy composite magnetic core.

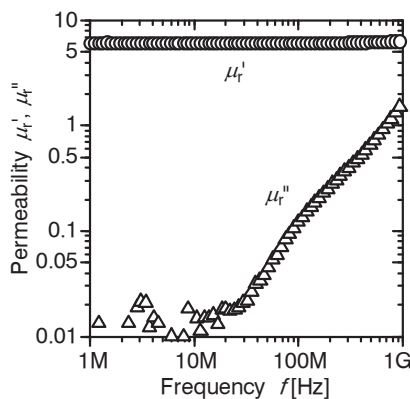


Fig. 2 Complex relative permeability of surface-oxidized carbonyl-iron powder/epoxy composite magnetic core.

(Agilent; 4291B) and a coaxial waveguide. The real part of the complex relative permeability μ_r' was low as about 6, but the imaginary part μ_r'' was as small as 10^{-2} order at 10 MHz or less. Although not measured below 1 MHz in frequency, the relative permeability μ_r' of about 6 was considered to be constant at hundreds kHz band and the magnetic loss μ_r'' was considered to be small enough at same hundreds kHz band.

The volume resistivity of the surface-oxidized carbonyl-iron powder/epoxy composite magnetic core was about $100 \Omega \cdot \text{m}^4$, which was 100 times higher than that of Mn-Zn ferrite core. Therefore, it was considered that the eddy current loss of the transformer core could be significantly suppressed at least up to 10 MHz.

2.2 Transformer structure

The output voltage of the quasi-resonant mode flyback-type DC-DC converter is controlled by changing both the on pulse width and the switching frequency according to the output current⁷⁾. As the output power becomes larger, the on pulse width expands and the switching frequency decreases. Also, the soft switching operation can be realized by using the resonance of the drain-source voltage of the MOSFET due to the inductance of the transformer primary winding and the capacitor connected in parallel to the MOSFET. Therefore, in order to increase the switching frequency, it is necessary to reduce the inductance of the primary winding. Since the composite magnetic core under investigation has a high saturation magnetization and the operating range ΔB of the transformer can be enlarged, even when the switching frequency decreases under heavy load, the magnetic saturation occurs hardly, which is due to the low inductance (low permeability composite magnetic core).

Fig. 3 shows the composite magnetic core transformer structure under investigation in this paper. The transformer winding was embedded in the composite magnetic core with a 30 mm-square size and

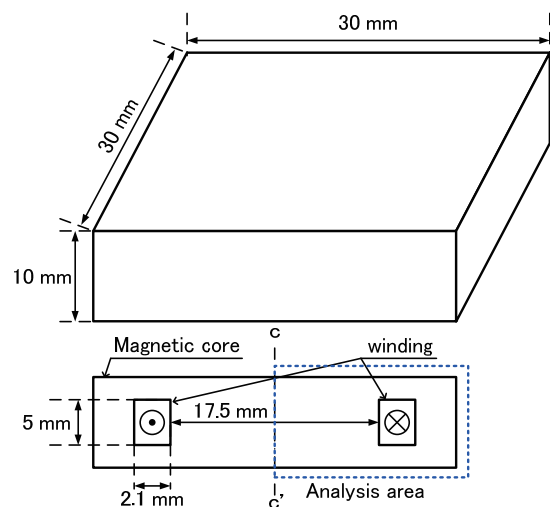


Fig. 3 Composite magnetic core transformer with embedded windings.

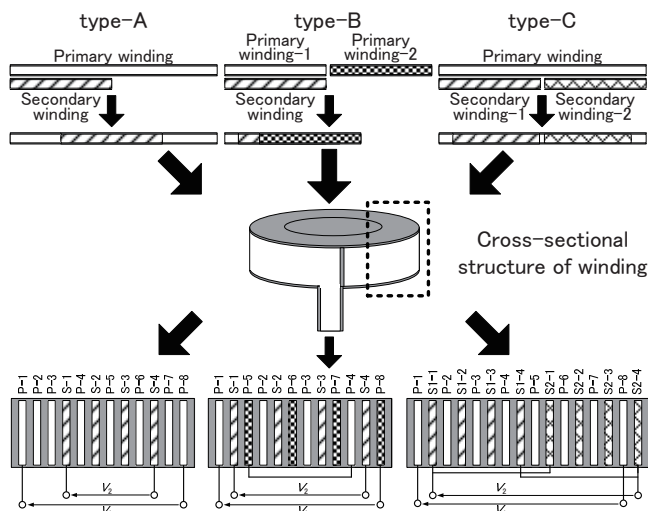


Fig. 4 Three types of winding layouts for composite magnetic core transformers with embedded windings.

10 mm in thickness. A copper-clad polyimide tape having a 70 μm thick, 5 mm wide copper conductor line formed on a 100 μm thick, 5.2 mm wide polyimide tape was used as the primary and secondary winding.

In this paper, inductance of the primary winding was designed so that the switching frequency was about 500 kHz when the converter output power of 60 W⁽⁸⁾. For a reason of the fabrication process of the tape wound coil, the number of turns was determined to be an even number, the primary winding turn was 8, and the secondary winding turn was 4. Since the composite magnetic core had a low relative permeability, winding layout becomes more important than when using other magnetic core materials having a high relative permeability. In general, when the primary and secondary winding were wound in an interleaved structure, the coupling coefficient between the windings could be increased⁽⁹⁻¹¹⁾. It was easy to wind in an interleaved structure when the number of turns of primary winding and that of secondary windings were equal. However, since the number of turns of primary and secondary winding of the transformer discussed in this paper was different, three types of transformers having different winding layout as shown in Fig. 4 were studied. In the cross-sectional view of windings in the lower figure of Fig. 4, “P-1” to “P-8” means from first turn to eighth turn of the primary winding, respectively. Similarly, “S-1” to “S-4” means from first turn to fourth turn of the secondary winding, respectively.

Type-A transformer consisted of one primary winding and one secondary winding. The secondary winding was concentratedly laid out near the center of the primary winding when looking at the cross-sectional structure of the windings. Therefore, the innermost conductors of the primary winding and the secondary winding were not adjacent to each other.

Type-B transformer consisted of two primary windings and one secondary winding. The secondary winding was sandwiched between two primary windings

and wound four turns. In order to make the primary winding eight turns, the winding end of one of the two primary windings and the winding start of the other were connected in series outside the magnetic core. Hence, the innermost conductors of the primary winding and the secondary winding were adjacent to each other, and the secondary winding were distributed and evenly laid out between the primary winding when looking at the cross-sectional structure of the windings.

Type-C transformer consisted of one primary winding and two secondary windings. After the first secondary winding was wound four turns with the primary winding, the second secondary winding was wound continuously four turns with the primary winding. In order to make the secondary winding four turns, two secondary windings were connected in parallel outside the magnetic core. As shown in Fig. 4, the innermost conductors of the primary winding and the secondary winding were adjacent to each other and the secondary winding of type-C were alternately and evenly laid out between the primary winding when looking at the cross-sectional structure of the windings. The inductance and the resistance of the two secondary windings were different because the lengths and inner diameters were different. Hence, it was considered that an imbalance in the current flowing of the two secondary windings may occurs. The following 2D-FEA numerical simulation and experiments took this behavior into account.

2.3 Fabrication procedure of composite magnetic core transformer

The fabrication procedure of the composite magnetic core transformer is as follows. An air-core winding having an inner diameter of 17.5 mm was fabricated. Air-core windings were covered with polyimide tape to prevent contact between the winding and the composite magnetic core material. The composite slurry was prepared by mixing surface-oxidized carbonyl-iron powder and two component epoxy precursor solution. The slurry was filled in a mold in which the winding was arranged and then cured at 120 degrees-C for 5 h. Thereafter, the size of the composite magnetic core was adjusted by polishing. As the lead wire from the winding inside the composite magnetic core, the same copper-clad polyimide tape was used.

3. Operation analysis for composite magnetic core transformer

3.1 Analysis model and conditions

In order to clarify the operation characteristics of the three types of transformers, 2D-FEA numerical simulation (Ansys; Maxwell) was introduced. As shown in Fig. 3, the analytical region was set to be the right half of the transformer cross section because of the symmetry of the device structure. The analytical model for deriving various parameters was a model rotated

Table 1 Parameters for 2D-FEA numerical simulation for three types of composite magnetic core transformers.

Material	Constant
Composite magnetic core	Permeability: $\mu_r' = 6$ (const.) Loss tangent: $\tan\delta = 0.002$ (const.) Conductivity: 0.01 S/m ($100 \Omega \bullet m$)
Conductor line (Copper)	Conductivity: 5.8×10^7 S/m Thickness: $70 \mu m$, Width: 5 mm
Insulator layer (Polyimide)	Conductivity: 0 S/m Thickness: $100 \mu m$, Width: 5.2 mm

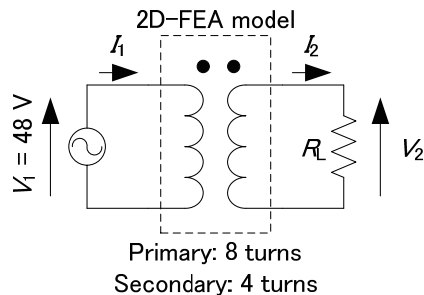


Fig. 5 Relationship between 2D-FEA numerical simulation for composite magnetic core transformer and equivalent circuit.

one time around $c-c'$ by post processing of the simulator. For this reason, the transformer core of the analytical model had a cylindrical shape with a diameter of 30 mm and a thickness of 10 mm, and the outer shape was different from the fabricated transformer. However, it was considered that there was little influence on the analysis result since the magnetic circuit of the transformer core had almost the same structure. The 2D-FEA could not accurately simulate the three-dimensional structure of the transformer including the influence of the lead wire etc. Therefore, quantitative consideration was difficult. However, it was considered sufficient to consider the relationship between the winding layout of the transformer and its operating characteristics under the same magnetic circuit structural condition.

Table 1 shows the properties used for analysis. The copper loss of the winding was calculated with taking the losses due to the skin effect and the proximity effect into account. The magnetic properties of the composite magnetic core were regarded as linear, and the magnetic hysteresis was not considered. The core loss was calculated from the imaginary part of the complex permeability shown in Fig. 2 and set as the loss tangent $\tan\delta (= \mu_r'' / \mu_r')$ in the 2D-FEA numerical simulation. Since the measurement variation of the imaginary part of complex permeability in the low frequency below 10 MHz was large, the value of $\tan\delta$ at 10 MHz was also used for the analysis below 10 MHz. Analysis was carried out under the constant voltage source excitation by using “Maxwell Circuit Editor” function capable of coupled analysis of FEA and the circuit simulation, the circuit diagram as shown in Fig. 5 was introduced, and

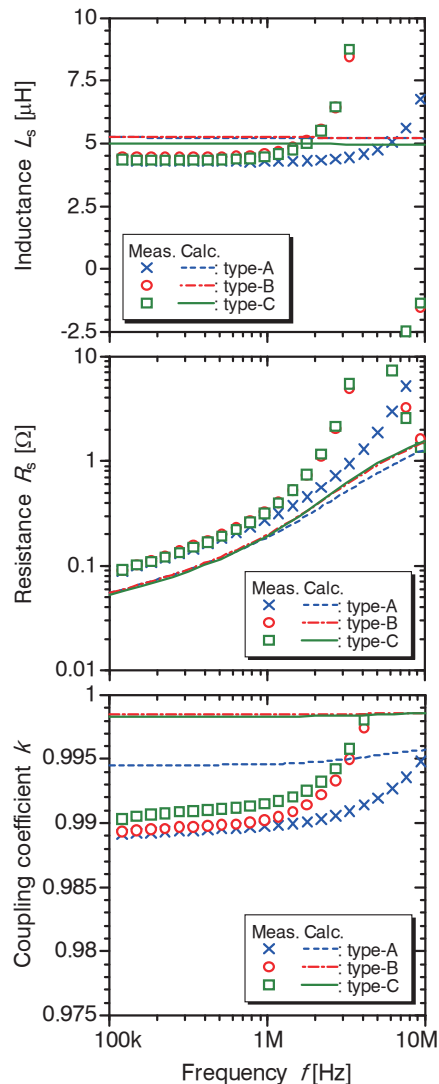


Fig. 6 Frequency characteristics of three types of transformers.

the operation characteristics of the transformers were simulated. In Fig. 5, a sinusoidal voltage source was connected to the primary side of the transformer, and a resistive load was connected to the secondary side. The input voltage V_1 was set to $48 V_{rms}$.

Since the measured value of the relative permeability in Fig. 2 was a small signal characteristic and $\tan\delta$ was regarded as constant value, the calculated power loss may be estimated to be smaller than the actual power loss. However, for the purpose of comparing the differences in characteristics due to the winding layout, the essential problem was considered to be small.

3.2 Electrical characteristics

Fig. 6 shows the equivalent series inductance, equivalent series resistance and coupling coefficient of the primary side of the transformer at the time of no-load. In Fig. 6, the plots are measured values by using an impedance/gain-phase analyzer (Agilent; 4194A) and the solid lines are calculated ones. The

Table 2 Measured and calculated DC resistance of each winding of transformers.

		Measured	Calculated
type-A	Primary	26.6 mΩ	24.0 mΩ
	Secondary	14.5 mΩ	12.1 mΩ
type-B	Primary	28.8 mΩ	24.1 mΩ
	Secondary	14.8 mΩ	12.0 mΩ
type-C	Primary	27.4 mΩ	24.7 mΩ
	Secondary	7.2 mΩ	6.3 mΩ

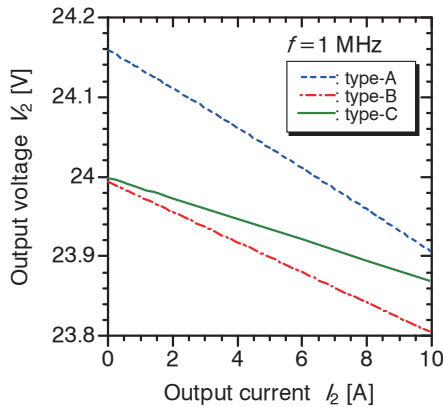


Fig. 7 Analysis results of load current dependence of output voltage for three types of transformers.

coupling coefficient was obtained by the secondary side open/short circuit method.

As shown in Fig.6, the equivalent series inductance of the fabricated transformer was about 4.6 μH regardless of the winding layout. The self-resonance frequency of type-B and type-C was lower than that of type-A because of the parasitic capacitance increase due to the winding layout⁵⁾.

Table 2 shows the measured and calculated DC resistance of each winding of the transformers. As shown in Table 2, the DC resistance of the primary windings was almost equal regardless of the winding layout. However, since two windings were connected in parallel, the DC resistance of the secondary winding of type-C was almost half.

Although there was the difference between the measured values and the calculated ones of each parameter, this was considered to be due to the positional deviation of the winding in the thickness direction of the magnetic core⁵⁾ and the influence of the parasitic parameters of the lead wire from the winding inside the composite magnetic core not considered in the analytical model. Also, since 2D-FEA was only magnetic field analysis, the influence of self-resonance did not appear in the calculation results. However, the tendency of the electrical characteristics of the three transformers generally agrees with the measured values and the calculated ones, it was considered that it was possible to compare the difference in characteristics due to the winding layout.

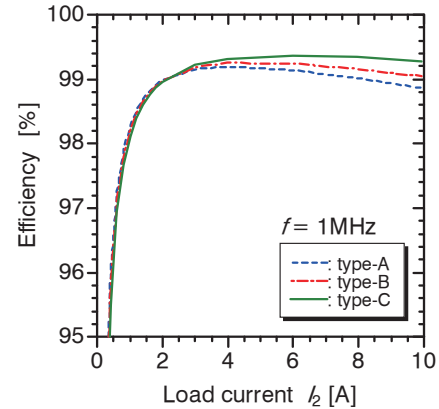


Fig. 8 Analysis results of load current dependence of efficiency for three types of transformers.

3.3 Load current dependences of transformer

Fig. 7 shows the calculated load current dependence of the output voltage V_2 of transformer. As shown in Fig. 7, the output voltage V_2 of type-A exceeded 24 V in the no-load and light load, which was higher than the value calculated from the turn ratio of 8:4. It was considered to be due to the low relative permeability of the composite magnetic core. Since the relative permeability was low, the main magnetic flux was considered not only to have the component in the composite magnetic core body but also to include the leakage component in the region near to the primary winding. As a result, the effective inner diameter of the secondary winding was considered to be enlarged and the inductance also increased. This was equivalent to the increase of the number of turns of the secondary winding. Hence, it was considered that the output voltage became higher than the value calculated from the turn ratio of 8:4. This operation suggests that the operating point of the transformer may unintentionally change from the operating point designed based on the specifications of the converter. On the other hand, in type-B and type-C, since the innermost conductors of the primary winding and the secondary winding were adjacent to each other and there was almost no difference in inner diameter, the output voltage was almost equal to the calculated value from the turn ratio of 8:4.

The output voltage of type-A transformer decreased more than the other two types of transformers. It was considered because type-A had lower coupling coefficient between primary and secondary winding than the other two types of transformers, and its leakage inductance was larger than the other two transformers.

3.4 Power efficiency and loss

Fig. 8 shows the calculated power efficiency of the transformer at 1 MHz. The maximum efficiency of 99% or more in any transformer was obtained. Since the loss due to the excitation current was mainly at no-load and light load, the type-A transformer with the lowest

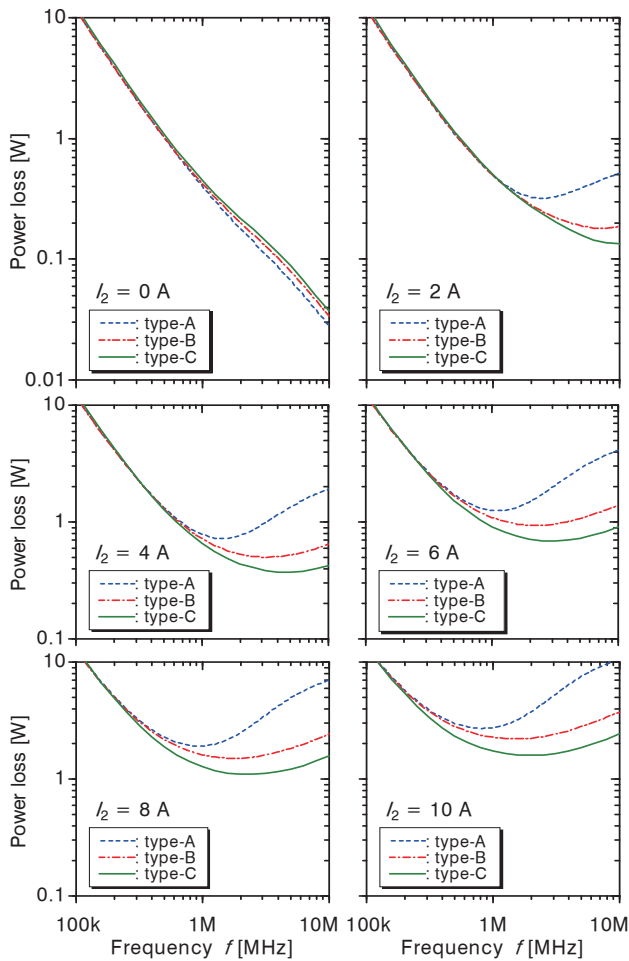


Fig. 9 Analysis results of frequency dependence of power loss for three types of transformers.

equivalent series resistance of primary winding at 1 MHz had the highest power efficiency. On the other hand, at heavy load, type-C with lowest secondary winding resistance and highest coupling coefficient between windings had the highest power efficiency.

Fig. 9 shows the calculated values of the frequency dependence of the power loss of the transformer. The frequency at the minimum power loss varied with the load current value, and the composite magnetic core transformers under investigation in this study exhibited the minimum power loss obtained at 500 kHz to 2 MHz according to the load current intending for the PFM controlled quasi-resonant type flyback converter in this study. The power loss in the low frequency increased because the winding loss increased and the input power factor decreased, which was considered to be owing to the low inductance and the increase of excitation current with lowering frequency. On the other hand, it was considered that the power loss increased in the high frequency due to the skin effect and proximity effect of the windings.

With increasing load current I_2 , the frequency at the minimum power loss shifted to the low frequency side in any transformer. In the quasi-resonant mode flyback-type DC-DC converter, since the switching

frequency decreases with increasing load current, there is a possibility that high efficiency can be maintained in the wide load condition when the composite magnetic core transformer is applied to such converter.

3.5 Magnetic flux density distribution in transformer

Fig. 10 shows the calculated magnetic flux density distribution of the three types of transformers when the frequency of 1 MHz and load current of 10 A. In Fig. 10, the in-phase flux component with the exciting current and 90-degrees phase-lag component are shown, where the stored energy in the transformer corresponds to the in-phase flux component and the energy loss corresponds to the 90-degrees phase-lag component. Since the magnetic loss due to $\tan\delta (= \mu_r'' / \mu_r')$ of the composite magnetic core was considered to be small enough at 1 MHz, the energy loss was considered to be mainly due to the windings.

From upper figure in Fig. 10, it was found that the in-phase magnetic flux density with the exciting current occurred mainly inside the winding and its spatial distribution was almost same in three types of winding layouts. On the other hand, as shown in the lower figure in Fig. 10, 90-degrees phase-lag magnetic flux density component shows a difference depending on the winding layout. In the type-A, 90-degrees phase-lag magnetic flux density distribution was generated between the conductors where the primary winding and the secondary winding were adjacent to each other. In particular, the magnetic flux was also distributed in the composite magnetic core at the beginning and the end of the secondary winding. Also in type-B, 90-degrees phase-lag magnetic flux was generated between the conductors where the primary winding and the secondary winding were adjacent to each other, but no 90-degrees phase-lag magnetic flux was generated in the composite magnetic core. Type-C had little 90-degrees phase-lag magnetic flux in the composite magnetic core and the 90-degrees phase-lag magnetic flux density between windings was smaller than type-B. It was considered that the 90-degrees phase-lag magnetic flux density component was due to the energy loss owing to the difference between the primary magnetomotive force and the secondary magnetomotive force. It was suggested that offsetting both the magnetomotive forces was incomplete in type-A. Furthermore, the leakage magnetic flux due to the offset magnetomotive force was considered to be a cause of an increase in eddy current loss in the winding. Therefore, it was inferred that type-A had larger winding loss at the large offset magnetomotive force when the heavy load, compared with the other two types of transformers. It was considered that the difference between the losses of type-B and type-C was not only due to the winding resistance of the secondary winding but also due to the influence of the eddy current loss caused by the leakage magnetic flux.

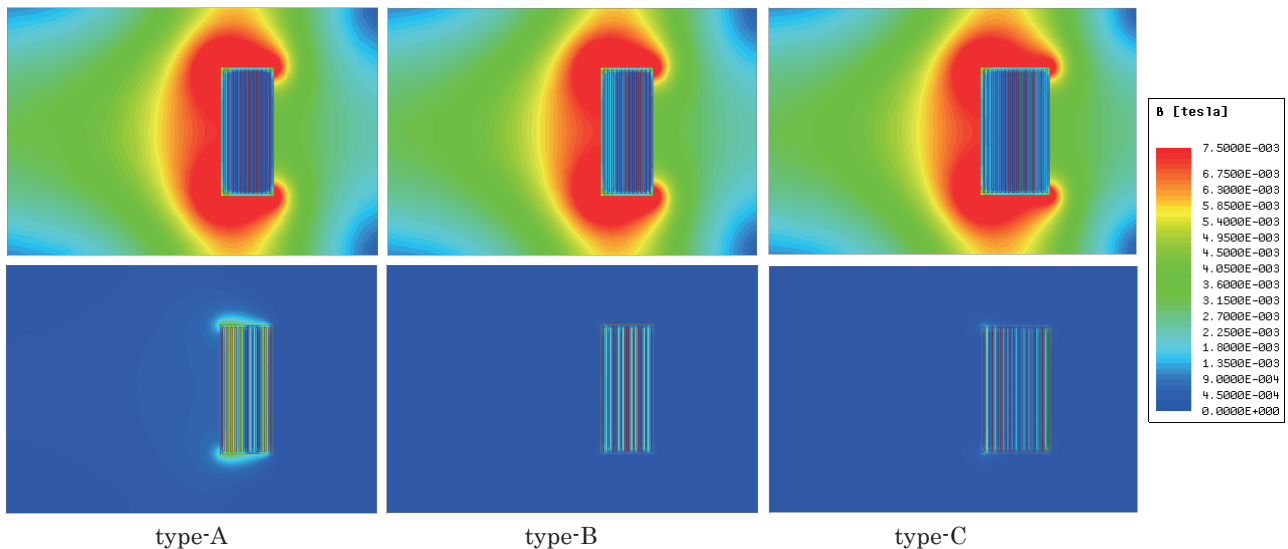


Fig. 10 Magnetic flux density distributions of three types of transformers. Upper figure represents in-phase flux component with exciting current, and lower figure shows flux component with 90-degree phase-lag from exciting current when frequency was 1 MHz and load current was 10 A.

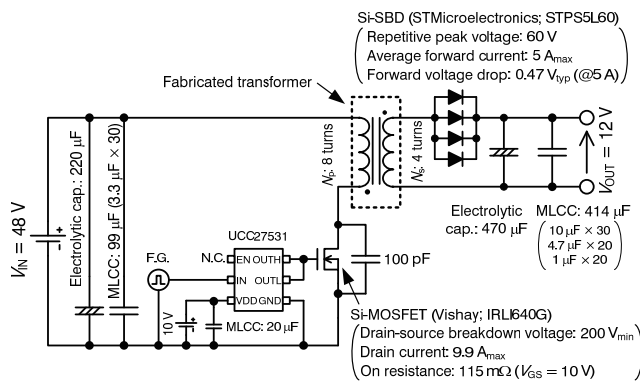


Fig. 11 Circuit diagram of PFM controlled quasi-resonant mode flyback-type DC-DC converter.

4. Application to PFM controlled quasi-resonant mode flyback-type DC-DC converter

4.1 Evaluation circuit diagram and conditions

Since the PFM controlled quasi-resonant mode flyback-type DC-DC converter⁷⁾ used in this study operates under the critical current mode and soft switching operation, it is expected to realize both higher conversion efficiency and higher switching frequency.

Fig. 11 shows the circuit diagram of the PFM controlled quasi-resonant mode flyback-type DC-DC converter with the composite magnetic core transformer under investigation. While the drain-source voltage waveform of the MOSFET was being confirmed with the oscilloscope, the switching frequency and on-time ratio were adjusted by the function generator (YOKOGAWA; FG420) so that the output voltage was constant at 12 V even if the output current was changed.

4.2 Experimental results and discussion

Fig. 12 shows the measured power conversion

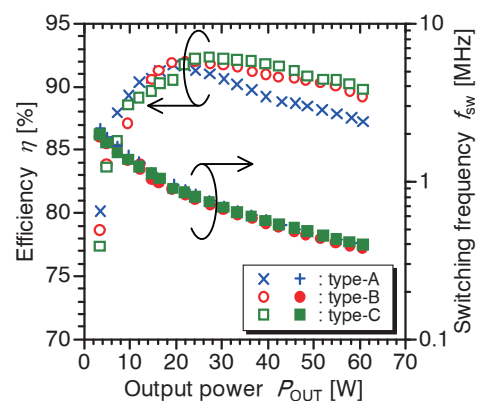


Fig. 12 Power conversion efficiency and switching frequency of converter using composite magnetic core transformers with different winding layouts.

efficiency and switching frequency of the converter using three types of composite magnetic core transformers. In this evaluation condition, the switching frequency varied from approximately 400 kHz to 2 MHz, which was roughly in agreement with the frequency band in which the power loss of the composite magnetic core transformer was small in the above-described operation analysis for the transformers. As shown in Fig. 12, when type-C was used, the maximum power conversion efficiency was 92.5% at an output power of around 28 W, and an efficiency of 90% was obtained at an output power of 60 W.

Power conversion efficiency at the light load was highest when type-A was used. However, with increasing the output power, the power conversion efficiency decreased significantly. Main reason of the efficiency decrease at large output power condition was considered to be owing to the increase of eddy current loss in the winding, where the leakage flux generated by the difference of the magnetomotive forces between

primary and secondary winding became large when heavy load condition. On the other hand, in type-B and type-C, the decrease in power conversion efficiency was small even if the output power increases. These trends were consistent with the results of power loss analysis for the transformers.

5. Conclusion

In general, the low permeability magnetic core is not suitable for transformer because of large leakage inductance owing to the low coupling coefficient between windings. Though the surface-oxidized carbonyl-iron powder/epoxy composite magnetic core has a low relative permeability of about 6, its magnetic loss was small below 10 MHz in frequency.

This study was done to develop the surface-oxidized carbonyl-iron powder/epoxy composite magnetic core transformer with high coupling coefficient and to apply it to the PFM controlled quasi-resonant mode flyback-type DC-DC converter. The obtained results are as follows.

(1) In order to obtain high coupling coefficient, the embedded winding structure was introduced to the composite magnetic core transformer design, and the three kinds of winding layouts were investigated on the bases of 2D-FEA numerical simulation and experiments. The adjacent layout of the primary and secondary winding was best choice for highest coupling coefficient over 0.99.

(2) The output voltage of the transformer, in which the innermost of the primary winding and the secondary winding were not adjacent to each other and had low coupling coefficient, was higher than the value calculated from the turn ratio at the no-load and light load. This operation suggests that the operating point of the transformer may unintentionally change from the operating point designed based on the specifications of the converter.

(3) The frequency at the minimum power loss shifted to the low frequency side with increasing load current in any transformer under investigation in this study, and the transformers exhibited the minimum power loss obtained at 500 kHz to 2 MHz according to the load current intending for the PFM controlled quasi-resonant type flyback converter in this study. Since the switching frequency of the converter decreases with increasing load current, there is a possibility that high efficiency can be maintained in the wide load condition when the composite magnetic core transformer is applied to such converter.

(4) Application of the fabricated composite magnetic core transformer with the best winding layout described in above (1) to the 48 V input/12 V output PFM controlled quasi-resonant mode flyback-type DC-DC converter exhibited a maximum power conversion efficiency of 92.5% at an output power of around 28 W, and 90% efficiency was obtained at an output power of 60 W. The obtained efficiency characteristics were consistent with the trend of power loss analysis for the composite magnetic core transformers.

Acknowledgements This study was supported in part by Grant-in-Aids for Japan Society for the Promotion of Science (15H02233), New Energy and Industrial Technology Development Organization (15101041-0), Japan, and Japan Science and Technology Agency (Nagano Satellite Cluster, Kyoto Super Cluster Program).

References

- 1) A. León-Masich, H. Valderrama-Blavi, J. M. Bosque-Moncusí, and L. Martínez-Salamero: *IET Power Electronics*, **8**, 6, pp.869-878 (2015).
- 2) H. Wang, A. M. H. Kwan, Q. Jiang, and K. J. Chen: *IEEE Trans. Electron Devices*, **62**, 4, pp.1143-1149 (2015).
- 3) M. Harrison: Plenary session, *IEEE Applied Power Electronics Conf. and Expo. (APEC) 2016*, Long Beach, CA, USA (2016).
- 4) K. Sugimura, Y. Miyajima, M. Sonehara, T. Sato, F. Hayashi, N. Zettsu, K. Teshima and M. Mizusaki: *AIP Advances*, **6**, 055932-1-8 (2016).
- 5) D. Shibamoto, A. Ueno, K. Sugimura, R. Hirayama, K. Sato, T. Sato, and M. Sonehara: *The Papers of Joint Technical Meeting on "Magnetics" and "Linear Drives"*, MAG-16-041/LD-16-033, pp.17-22 (2016) (in Japanese).
- 6) K. Sato, K. Sugimura, T. Sato, M. Sonehara, and H. Takeuchi: *T. Magn. Soc. Jpn. (Special Issues)*, **1**, pp.44-52 (2017) (in Japanese).
- 7) Y. Asako, H. Shiroyama, Y. Ishizuka, H. Matsuo: *IEICE Technical Report*, EE2007-64/CPM2007-149, pp.1-6 (2008) (in Japanese).
- 8) J. Togawa: *Suicching-dengen no koiru/toransu sekkei* (in Japanese), pp.201-209 (CQ shuppansha, Tokyo, 2012).
- 9) T. Sato, H. Yokoyama, K. Yamasawa, K. Toya, S. Kobayashi, T. Minamisawa: *T. IEE Japan*, **120-A**, 3, pp.266-271 (2000) (in Japanese).
- 10) Z. Ouyang, J. Zhang, W. G. Hurley: *IEEE Trans. Power Electronics*, **30**, 10, pp.5769-5775 (2015).
- 11) H. Tanaka, K. Nakamura, O. Ichinokura: *J. Magn. Soc. Jpn.*, **40**, pp.35-38 (2016).

Received June 13, 2017; Revised July 10, 2017; Accepted July 24, 2017